

Towards very high-order accurate schemes for unsteady convection problems on unstructured meshes

R. Abgrall^{1,2,*}, N. Andrianov² and M. Mezhine^{2,‡}

¹*Institut Universitaire de France, France*

²*Mathématiques Appliquées de Bordeaux, Université Bordeaux I, 351 cours de la Libération, 33405 Talence, France*

SUMMARY

We construct several high-order residual-distribution methods for two-dimensional unsteady scalar advection on triangular unstructured meshes. For the first class of methods, we interpolate the solution in the space–time element. We start by calculating the first-order node residuals, then we calculate the high-order cell residual, and modify the first-order residuals to obtain high accuracy. For the second class of methods, we interpolate the solution in space only, and use high-order finite difference approximation for the time derivative. In doing so, we arrive at a multistep residual-distribution scheme. We illustrate the performance of both methods on several standard test problems. Copyright © 2005 John Wiley & Sons, Ltd.

KEY WORDS: residual-distribution schemes; fluctuation splitting schemes; unstructured meshes; hyperbolic problems

1. INTRODUCTION

The topic of this article is the approximation of linear and nonlinear time-dependent hyperbolic problems on unstructured meshes. Although we concentrate here on the 2D case, the extension to 3D is straightforward. Also, we provide several 1D numerical illustrations. We consider

* Correspondence to: R. Abgrall, Mathématiques Appliquées de Bordeaux, Université Bordeaux I, 351 cours de la Libération, 33405 Talence, France.

† E-mail: remi.abgrall@math.u-bordeaux.fr

‡ Present affiliation: NUMECA International, avenue Franklin Roosevelt 5, 1050 Brussels, Belgium.

Contract/grant sponsor: HYKE; contract/grant number: HPRN-CT-2002-00282

Received 27 April 2004

Revised 15 November 2004

Accepted 16 November 2004

the following model problem for the scalar unknown u :

$$\begin{aligned} \frac{\partial u}{\partial t} + \frac{\partial f(u)}{\partial x} + \frac{\partial g(u)}{\partial y} &= 0, & x \in \Omega \subset \mathbb{R}^2 \\ u(x, t) &= u_b(x, t) & \text{on the inflow part of } \partial\Omega \\ u(x, 0) &= u_0(x) & \text{at } t = 0 \end{aligned} \tag{1}$$

In what follows, we will consider the advection $(f, g) = \lambda u$, and the 1D and 2D Burgers equation $(f, g) = (\frac{u^2}{2}, 0)$, $(f, g) = (\frac{u^2}{2}, u)$.

In this work, we are interested in the so-called residual-distribution (RD) or fluctuation splitting schemes introduced by Deconinck *et al.* [1]. These methods can be seen as finite element methods where the artificial dissipation is tuned according to ideas coming from the finite difference high-resolution context. The RD methods use a continuous representation of the unknowns and have the most possible compact stencil among the discontinuous Galerkin or finite volume methods. This latter property is advantageous for parallelization and for high-order extensions.

This paper contains preliminary results on stabilized very high-order RD schemes for (1). In Section 2, we recall several results on the second-order RD scheme for unsteady problems, described in Reference [2]. In Section 3, we introduce two versions of higher-order extension of this RD scheme. Finally, Section 4 contains some numerical examples.

Throughout the paper, we will consider a triangulation of Ω , consisting of generic triangles T_j with characteristic size h , $j = 1, \dots, n_t$. The vertices of a triangle T are denoted by M_{i_1} , M_{i_2} , M_{i_3} or simply by 1, 2, 3 if no ambiguity occurs. The time step is Δt and $t_n = n\Delta t$. The approximate solution to (1) is denoted by $u^h(x, t)$ and its values at (M_j, t_n) by u_j^n .

2. RESIDUAL DISTRIBUTION SCHEMES, SECOND-ORDER UNSTEADY CASE

For simplicity, we consider here problem (1) with a constant advection speed. Starting from a triangle T , we define the space–time prism $K = T \times [t_n, t_{n+1}]$. The numerical solution of (1) is interpolated in K linearly in space and time:

$$u^h(x, t) = u^{n+1}(x) \frac{(t - t_n)}{\Delta t} + u^n(x) \frac{(t_{n+1} - t)}{\Delta t} \tag{2}$$

where u^n and u^{n+1} are linear interpolations between $\{u_{j_1}^n, u_{j_2}^n, u_{j_3}^n\}$ and $\{u_{j_1}^{n+1}, u_{j_2}^{n+1}, u_{j_3}^{n+1}\}$, respectively. The total residual in K is defined as

$$\Phi^K := \int_{t_n}^{t_{n+1}} \int_T \left(\frac{\partial u^h}{\partial t} + \lambda \cdot \nabla u^h \right) dx dt \tag{3}$$

Introducing the inward scaled normal \mathbf{n}_i opposite to M_i in T , and setting $k_i = \frac{1}{2} \lambda \cdot \mathbf{n}_i$, we have

$$\Phi^K = \frac{|T|}{3} \sum_{j=1}^3 (u_j^{n+1} - u_j^n) + \frac{\Delta t}{2} \sum_{j=1}^3 k_j (u_j^{n+1} + u_j^n)$$

The idea of RD schemes is to split Φ^K into sub-residuals Φ_i^K , which are ‘sent’ by the prism K to its six vertices, and then to gather the sub-residuals for any vertex in order to update

the solution. The definition of the sub-residuals uses the causality principle: the past does not depend on the future. This means that only the sub-residuals sent by K to the vertices $(M_j, t_{n+1})_{j=1,3}$ may be non-zero. This enables one to decouple the time slabs. Then, conservation is guaranteed provided the following relation holds:

$$\sum_{(M_j, t_{n+1}) \in K} \Phi_j^K = \Phi^K \tag{4}$$

The RD scheme is then defined by

$$\sum_{K \ni (M_i, t_{n+1})} \Phi_i^K = 0 \tag{5}$$

Now we need to define the sub-residuals. In doing so, we wish to ensure certain stability and accuracy properties.

Stability requirements: Consider, as in [2]

$$\begin{aligned} \Phi_i^K &= \frac{|T|}{3}(u_i^{n+1} - u_i^n) + \frac{\Delta t}{2}(k_i^+(u_i^{n+1} - \tilde{u}^{n+1}) + k_i^+(u_i^n - \tilde{u}^n)) \\ \tilde{u}^n &= N \left(\sum_{j \in T} k_j^- u_j^n \right), \quad \tilde{u}^{n+1} = N \left(\sum_{j \in T} k_j^- u_j^{n+1} \right), \quad N = \left(\sum_{j \in T} k_j^- \right)^{-1} \end{aligned} \tag{6}$$

The N scheme (5), (6) leads to the system $Au^{n+1} = Bu^n$, where A and B are constant matrices. The analysis of Reference [2] shows that A is a monotone matrix whatever the time step Δt , and that B has positive entries provided $\Delta t \max_T \sum_{j \in T} k_j^+ / |T| \leq 1$. Therefore, the N scheme is L^∞ stable under the CFL-like condition. Numerical experiments show that the scheme remains monotone also when this condition is violated by a large factor. Also, the N scheme (5), (6) is *unconditionally* L^2 stable, see Reference [2] for details.

Following Ricchiutto [3], consider a variant of the N scheme:

$$\Phi_i^T = \frac{|T|}{3}(u_i^{n+1} - u_i^n) + \Delta t k_i^+(u_i^{n+1} - \tilde{u}^{n+1}) \tag{7}$$

In Appendix A, we show that scheme (5), (7) leads to the system $Au^{n+1} = u^n$, where A is a monotone matrix whatever the time step Δt . This guarantees *unconditional* L^∞ stability. Also, scheme (5), (7) is *unconditionally* L^2 stable; see Appendix A for details. Note that the sub-residuals (7) do not satisfy the conservation requirement (4).

Accuracy requirement: For smooth exact solutions to (1) and regular meshes, scheme (5) is formally second-order in space and time if for all prisms K the sub-residuals satisfy

$$\Phi_i^K = \mathcal{O}(h^3, \Delta t^3) \tag{8}$$

see References [2, 4]. Among several ways of fulfilling condition (8), the easiest one is the linearity preserving property; see References [1, 4]. It ensures that for regular meshes, the *distribution coefficients* $\beta_i = \Phi_i^K / \Phi^K$ are uniformly bounded independent of h and Δt .

It is known that it is impossible to have a linear scheme, i.e. the distribution coefficients β_i do not depend on u^h , which is both LP and L^∞ stable. In the next paragraph, we sketch construction schemes that satisfy both these properties.

Accuracy and stability: Consider a first-order monotone scheme (5) with residuals $\{\Phi_i^L\}$ and the corresponding distribution coefficients $\beta_i = \Phi_i^L/\Phi^K$. We wish to construct a second-order scheme (5) with $\{\Phi_i^H\}$ such that (i) the scheme is conservative, (ii) the scheme satisfies the maximum principle, and (iii) $\hat{\beta}_i = \Phi_i^H/\Phi^K$ are uniformly bounded in order to guarantee the LP condition (8). This approach is described in Reference [2] and originates from a remark of Sidilkover. He noticed that for steady scalar problems the condition $\Phi_i^H/\Phi_i^L \geq 0$ for any triangle T guarantees the maximum principle. Conservation requires that $\sum_j \Phi_j^L = \sum_j \Phi_j^H = \Phi^K$. Hence, the problem reduces to the construction of a mapping from $(\beta_1, \beta_2, \beta_3)$ to $(\hat{\beta}_1, \hat{\beta}_2, \hat{\beta}_3)$ such that (i) $\sum_i \beta_i = \sum_i \hat{\beta}_i = 1$ (conservation constraint), (ii) $\beta_i \hat{\beta}_i \geq 0, i = 1, 2, 3$ (monotonicity constraint), and (iii) $\hat{\beta}_i$ are bounded, $i = 1, 2, 3$ (LP constraint). In Reference [5], we have presented a geometrical interpretation of these conditions, and a systematic way of constructing the mapping. The simplest formula of the type is

$$\hat{\beta}_i = \frac{\beta_i^+}{\sum_j \beta_j^+}, \quad \beta_i^+ = \max(0, \beta_i) \quad (9)$$

Note that the division in (9) is always well defined because

$$\sum_j \beta_j^+ = 1 - \sum_j \hat{\beta}_j^- \geq 1 \quad (10)$$

The RD scheme is then defined by (5), the definition of Φ_i^L, Φ^K and the non-linear limiter (9). This leads to a non-linear scheme of the type $Au^{n+1} = Bu^n$, where now A and B depend on u^{n+1} and u^n . Efficiency requires that the time step be as large as possible. For the N scheme (6), we have the restriction on time step since it is L^∞ stable under the CFL-type condition. However, a number of degrees of freedom are still available. For example, one does not really need that the underlying first-order scheme Φ_i^L be conservative, since conservation is recovered for the second-order scheme Φ_i^H due to $\sum_j \beta_j = 1$. Thus, it is possible to use Ricchiuto's version of the N scheme (7) to define β_i , and use (9) to calculate $\hat{\beta}_i$. We still have a conservative scheme! However, one must be aware that property (10) is no longer valid, so that there is no guarantee that β_i are indeed well defined. In practice, we have never encountered this difficulty.

3. VERY HIGH-ORDER RESIDUAL DISTRIBUTION SCHEMES

In Reference [5], we have considered the very high-order discretization of the steady version of (1). Here, we extend this work to the unsteady case. We present two versions that differ by the time approximation in (1). In both cases, we consider a space-time element $K = T \times [t_n, t_{n+1}]$, and introduce a sub-triangulation of T as follows.

For each point $x \in T$, we introduce its barycentric co-ordinates (a, b, c) . As in Reference [5], from the points $M_i = \{i/p, j/p, (p-i-j)/p\}$, $0 \leq i, j \leq p$, we define a sub-triangulation of T , consisting of p^2 sub-triangles, see Figure 1 for the case $p=2$. We denote by T_ξ any of these p^2 sub-triangles, $K_\xi := T_\xi \times [t_n, t_{n+1}]$, and by σ any of the $(p+1)(p+2)/2$ degrees of freedom in T .

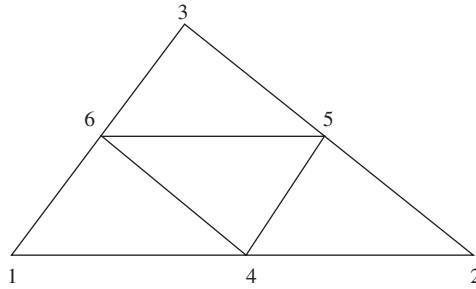


Figure 1. Sub-triangulation of T used for the quadratic interpolation.

Now, we can define the p th-order basis functions on the triangle T such that $\phi_l(M_m) = \delta_{lm}$, $\phi_l \in \mathbb{P}_p$, where δ_{lm} is the Kronecker symbol. The p th-order interpolation u^n at fixed time t^n is then

$$u^n = \sum_{l=1}^{(p+1)(p+2)/2} u^n(M_l) \phi_l \tag{11}$$

In order to construct an RD scheme, we need to split the total residual Φ^K into the sub-residuals ‘sent’ to the degrees of freedom of K . In doing so, we use the causality and conservation principles analogous to Section 2, i.e.

$$\Phi_{(\sigma, t_n)}^{K_\xi} := 0, \quad \Phi_{(\sigma, t_{n+1})}^K = \sum_{K_\xi \ni (\sigma, t_{n+1}), K_\xi \subset K} \Phi_\sigma^{K_\xi} \tag{12}$$

Then, the RD scheme is defined by

$$\sum_{K \ni (\sigma, t_{n+1})} \Phi_{(\sigma, t_{n+1})}^K = 0 \tag{13}$$

The accuracy of the scheme (13) is described by

Proposition 1

A necessary condition for scheme (13) to reach $(p + 1)$ th order in space and $(q + 1)$ th order in time, i.e. $u(x, t) - u_h(x, t) = \mathcal{O}(h^{p+1}, \Delta t^{q+1})$, where u is the smooth solution to (1), is that $\Phi_\sigma^K = \mathcal{O}(h^{p+1}, \Delta t^{q+1})$. This is true if u^h is polynomial of degree p in space and q in time.

The proof is similar to that of Reference [5] since we can consider (1) as a *steady* problem in \mathbb{R}^3 . Similar to Section 2, we construct the sub-residuals Φ_σ^K as follows:

1. For all sub-triangles T_ξ , (i) calculate the first-order sub-residuals $\Phi_{\sigma_1}^L, \Phi_{\sigma_2}^L, \Phi_{\sigma_3}^L$ by the N scheme (6) (or alternatively by Ricchiutto’s version (7)), (ii) compute Φ^{K_ξ} with high accuracy (see below), and (iii) compute high-order sub-residuals $\Phi_{\sigma_i}^H := \hat{\beta}_{\sigma_i} \Phi^{K_\xi}$ using

$$\hat{\beta}_{\sigma_i} = \frac{(\Phi_{\sigma_i}^L / \Phi^{K_\xi})^+}{\sum_{j=1}^3 (\Phi_{\sigma_j}^L / \Phi^{K_\xi})^+} \tag{14}$$

2. Accumulate contributions to Φ_σ^K from different sub-triangles $\Phi_{(\sigma, t_{n+1})}^K := \sum_{T_\xi \ni \sigma} \Phi_\sigma^{K_\xi}$.

The conservation condition (12) is satisfied by construction when $\sum_{i=1}^3 \hat{\beta}_{\sigma_i} = 1$. The scheme (13) is monotone since $\Phi_{\sigma}^L \Phi_{\sigma}^H \geq 0$. Considering how Φ_{σ}^L is constructed, this implies that the time step for the high-order scheme is constrained by the CFL-type condition of the low-order scheme. Finally, scheme (13) has a high order of accuracy since $\hat{\beta}_{\sigma_i}$ are bounded. Below, we describe two ways of computing the total residuals $\Phi^{K_{\xi}}$, which lead to different versions of scheme (13).

3.1. High-order space–time interpolation

Let p and q be two integers greater than 1. We consider the following interpolation in the space–time element K :

$$u^h(x, t) = L_{n-q+2}(t)u^{n-q+2}(x) + \dots + L_n(t)u^n(x) + L_{n+1}(t)u^{n+1}(x) \tag{15}$$

Here $L_{n-q+2}(t), \dots, L_{n+1}(t)$ are the Lagrange interpolants of degree q between the time levels t_{n-q+2} and t_{n+1} . The functions $u^{n-q+2}(x), \dots, u^{n+1}(x)$ are given by (11). Observe that we need the linear interpolation between the time levels t_n and t_{n+1} to get $u - u_h = \mathcal{O}(h^{p+1}, \Delta t^2)$, quadratic interpolation between the time levels t_{n-1}, t_n and t_{n+1} to get $u - u_h = \mathcal{O}(h^{p+1}, \Delta t^3)$ and so on. At each time level, we need $(p + 1)(p + 2)/2$ degrees of freedom for $(p + 1)$ th order of spatial accuracy.

Using the high-order space–time interpolation (15), we can compute the residual over K_{ξ}

$$\Phi^{K_{\xi}} = \int_{t_n}^{t_{n+1}} \int_{T_{\xi}} \left(\frac{\partial u^h}{\partial t} + \lambda \cdot \nabla u^h \right) dx dt \tag{16}$$

which basically consists of computing integrals of the form

$$\int_{T_{\xi}} u^n(x) dx, \quad \int_{T_{\xi}} \lambda \cdot \nabla u^n(x) dx, \quad \int_{t_n}^{t_{n+1}} L_n(t) dt \tag{17}$$

The first integral in (17) is evaluated using Gaussian quadrature in barycentric co-ordinates, the second by 1D Gaussian quadrature (after transformation to the integral over ∂T_{ξ} by Gauss’ theorem), and the third by a Newton–Cotes quadrature.

Below, we present several high-order approximations to the residual (16); they differ just in the order of Lagrange interpolants in (15) and the type of the Newton–Cotes quadrature formula used to approximate the time integral in (17).

Third order in time: If we use quadratic time interpolation in (15) together with the Simpson rule for the time integral in (17), the residual is $\mathcal{O}(h^{p+1}, \Delta t^4)$ with

$$\begin{aligned} \Phi^{K_{\xi}} &= \int_{T_{\xi}} (u^{n+1}(x) - u^n(x)) dx + \frac{5\Delta t}{12} \int_{T_{\xi}} \lambda \cdot \nabla u^{n+1}(x) dx \\ &+ \frac{2\Delta t}{3} \int_{T_{\xi}} \lambda \cdot \nabla u^n(x) dx - \frac{\Delta t}{12} \int_{T_{\xi}} \lambda \cdot \nabla u^{n-1}(x) dx \end{aligned} \tag{18}$$

Fourth order in time: If we use cubic time interpolation in (15) together with the $\frac{3}{8}$ rule for the time integral in (17), the residual is $\mathcal{O}(h^{p+1}, \Delta t^5)$ with

$$\begin{aligned} \Phi^{K_\xi} = & \int_{T_\xi} (u^{n+1}(x) - u^n(x)) \, dx + \frac{3\Delta t}{8} \int_{T_\xi} \lambda \cdot \nabla u^{n+1}(x) \, dx \\ & + \frac{19\Delta t}{24} \int_{T_\xi} \lambda \cdot \nabla u^n(x) \, dx - \frac{5\Delta t}{24} \int_{T_\xi} \lambda \cdot \nabla u^{n-1}(x) \, dx \\ & + \frac{\Delta t}{24} \int_{T_\xi} \lambda \cdot \nabla u^{n-2}(x) \, dx \end{aligned} \tag{19}$$

Observe that the RD scheme (13) with residuals (18) or (19) is a *multistep* RD scheme. Indeed, in order to update the solution at time level t_{n+1} , we will need to use the values of the solution from previous time levels. The number of these time levels depends on the temporal accuracy of scheme (13).

3.2. High-order finite difference in time

In the previous paragraph, the idea was first to reconstruct the solution and then to compute the prismatic residual exactly as was done in Reference [2]. Alternatively, one can approximate the time derivative in (1) by a high-order finite difference approximation, but still use high-order interpolation in space. For example, setting $\Delta u^n(x) := u^{n+1}(x) - u^n(x)$, one can approximate (1) with

$$(1 + \phi + \psi) \frac{\Delta u^n(x)}{\Delta t} - \phi \frac{\Delta u^{n-1}(x)}{\Delta t} - \psi \frac{\Delta u^{n-2}(x)}{\Delta t} + \lambda \cdot \nabla u^{n+1}(x) = 0 \tag{20}$$

This approximation is second-order accurate in time if $(\phi, \psi) = (\frac{1}{2}, 0)$ and third-order accurate if $(\phi, \psi) = (\frac{7}{6}, \frac{1}{3})$. We can view (20) as the *steady* problem for $x \in \mathbb{R}^2$:

$$\alpha u^{n+1}(x) + \lambda \cdot \nabla u^{n+1}(x) = S(x) \tag{21}$$

with $\alpha = (1 + \phi + \psi)/\Delta t$ and the ‘source term’ $S(x) = (1 + \phi + \psi)/\Delta t u^n(x) + \phi \Delta u^{n-1}(x)/\Delta t + \psi \Delta u^{n-2}(x)/\Delta t$. For the steady problem (21), we define the residual over the prism K_ξ as follows:

$$\Phi^{K_\xi} = \int_{T_\xi} (\alpha u^{n+1}(x) + \lambda \cdot \nabla u^{n+1}(x) - S(x)) \, dx \tag{22}$$

As in the previous paragraph, the RD scheme (13) with the residual (22) is a multistep RD scheme.

3.3. Comments on the numerical procedure

In both cases, the scheme writes $Au^{n+1} = Bu^n$, where matrices A and B both depend on u^{n+1} , u^n and Δt . The linear system is solved by a standard numerical procedure. Here we have chosen a Jacobi-like iterative method.

4. NUMERICAL EXAMPLES

We present several 1D and 2D examples; the 1D schemes are obtained from the ones presented here if one replaces triangles with intervals. In that case, the triangles are replaced by intervals with even indices $[2p, 2p + 2]$, $p \in \mathbb{Z}$, and the sub-triangles are $[2p, 2p + 1]$, $[2p + 1, 2p + 2]$. We have always used schemes which are third-order in space.

4.1. One-dimensional examples

Here use the space–time interpolation method of Section 3.1 for the 1D version of (1) with $\lambda = 1$ and the initial data

$$u_0(x) = 1 + \cos(4\pi(x - 0.35)) \quad \text{if } x \in [0.1, 0.6] \quad 0 \quad \text{else} \quad (23)$$

in $[0, 1]$ or with the initial condition

$$u_0(x) = \begin{cases} 1 & \text{if } x \leq 0.5 \\ 0 & \text{else} \end{cases} \quad (24)$$

The solutions are represented in Figures 2 and 4, the L^1 and L^2 errors in Figure 3. A CFL number of 0.5 is used with 101 mesh points over 101 time steps.

We have also considered the Burgers equation with the initial conditions

$$u_0(x) = \begin{cases} -1 & \text{if } x \leq 0.5 \\ 0.1 & \text{else} \end{cases} \quad (25)$$

which gives a fan

$$u_0(x) = \begin{cases} -0.1 & \text{if } x \leq 0.5 \\ 1 & \text{else} \end{cases} \quad (26)$$

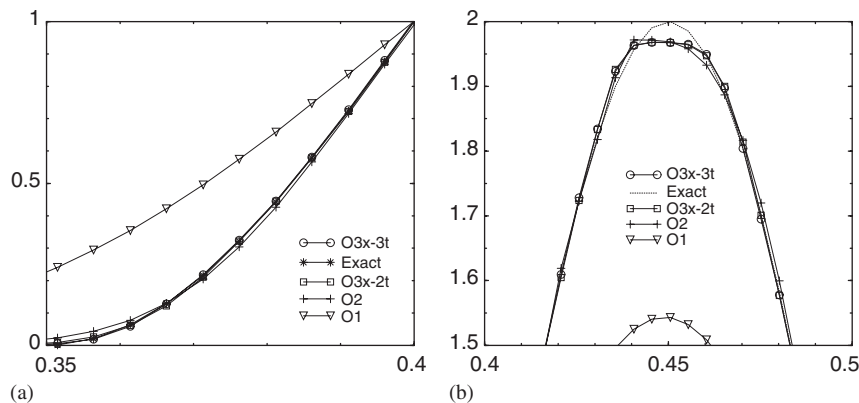


Figure 2. Zooms of the solution of the transport problem with (23). Legend; $O3x-3t$: third-order in time and space; $O3x-2t$: third-order in space, second-order in time; $O2$: second-order; $O1$: first-order.

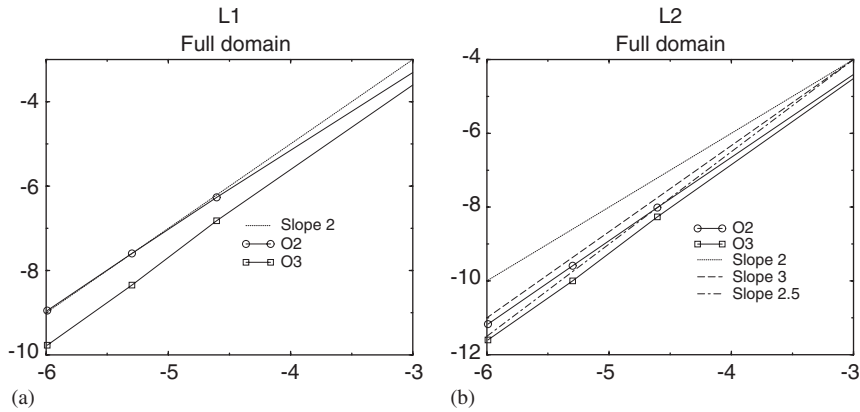


Figure 3. Error on $1 + \cos(4\pi(x - 0.35))$ if $x \in [0.1, 0.6]$, 0 else. (a) L^1 ; (b) L^2 .

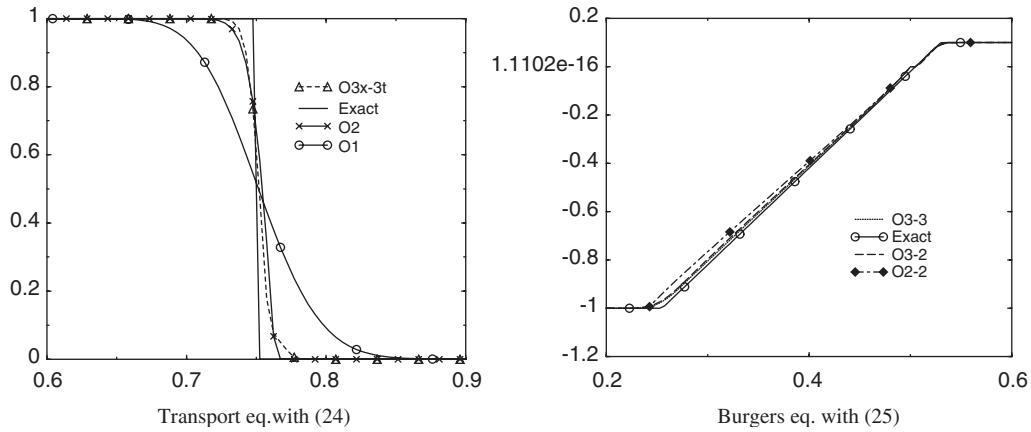


Figure 4. Solution for the nonsmooth initial conditions. $O3x - 3t$: third-order in time and space; $O3x - 2t$: third-order in space, second-order in time.

which gives a choc propagating at speed $u = 0.45$ to the right, and

$$u_0(x) = \sin(2\pi x) \tag{27}$$

for which a shock appears after time $t^* = \frac{1}{\pi}$.

In the case of the Burgers equation, we had to set up the following entropy conditions. If in a sub-cell $[x_j, x_{j+1}]$, where $j = 2p$ or $2p + 1$, we have $u_j u_{j+1} \leq 0$ (case of an expansion shock), the scheme reduces to first-order in that sub-cell. Since we are in 1D, this does not modify the conservation property of the scheme. Note that if the criterion is $u_j u_{j+1} \leq 0$ and $u_j \leq u_{j+1}$ as it should be, the second-order scheme works fine but the third-order one may produce a slight overshoot in Figure 4 (if the initial condition changes sign only), and for some Δx . The reason seems numerical, but we have not been able to find it (Figure 5).

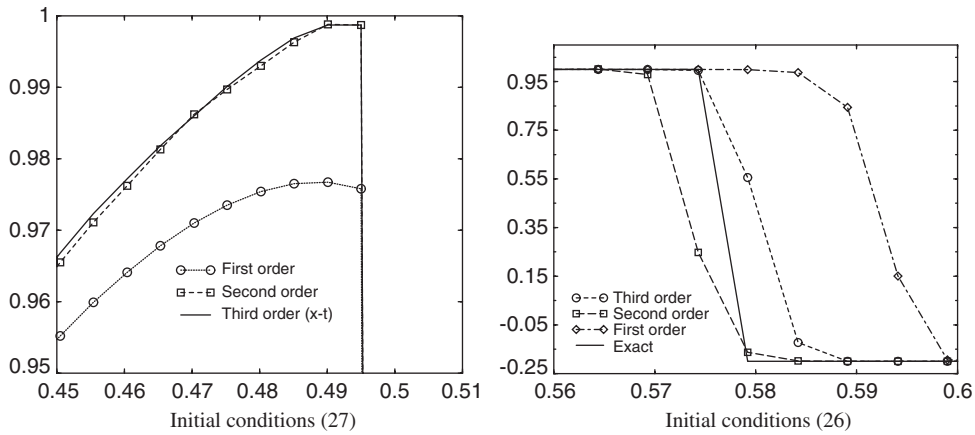


Figure 5. Zoom of the solution of the Burgers equation with (27) around $x = 0.5$. $O(3x - 3t)$: third-order in time and space; $O(3x - 2t)$: third-order in space, second-order in time.

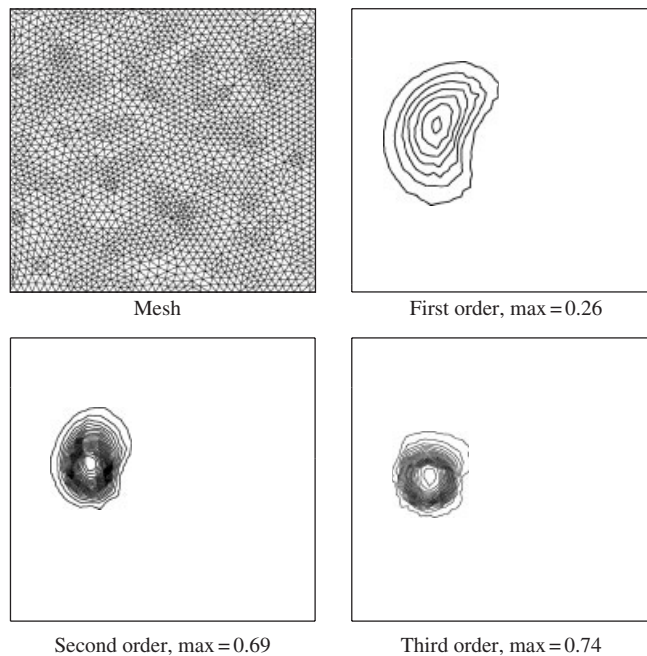


Figure 6. Results for the circular advection problem after one rotation. Initial condition: $u_0(x, y) = \max(1 - (r/2)^2, 0)$ with $r = \sqrt{(x - 0.5)^2 + y^2}$. The minimum value is always 0.

4.2. Two dimensional examples

We have run the scheme of Section 3.2 with second-order accuracy in time only based on Ricchiuto’s N scheme (7) and a CFL number set to 2. The scheme is unconditionally

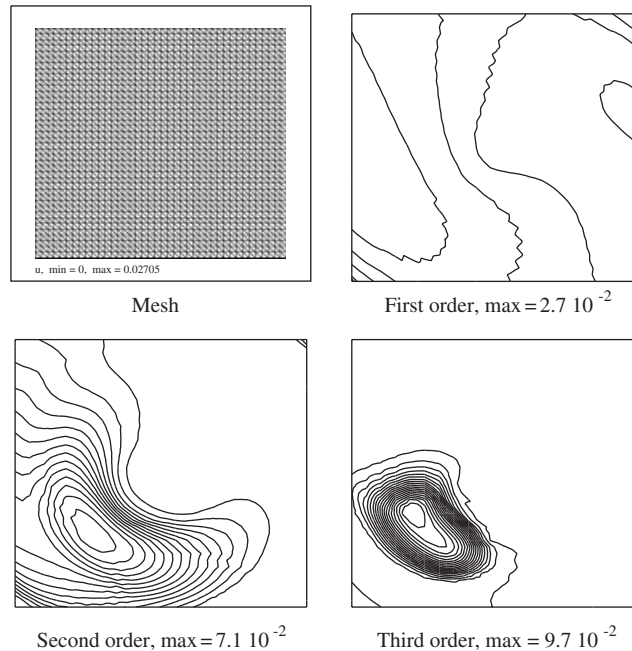


Figure 7. Results for the circular advection problem (ten rotations). The minimum value is always 0.

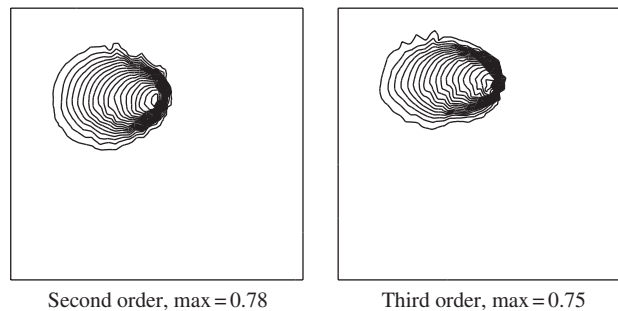


Figure 8. Results for the Burgers-like problem. The minimum value is always 0.

stable. The problem is the circular advection problem. The mesh is displayed in Figure 6. The initial condition is set to $u(x, y) = \max(1 - (r/2)^2, 0)$ where $r = \sqrt{(x + 0.5)^2 + y^2}$. The result is displayed in Figure 6 for the first-order scheme, $(p, q) = (1, 1)$ (second-order version of Reference [2]) and $(p, q) = (1, 2)$ (second-order in time, third-order in space), after one rotation. The CFL is set to 2. After ten rotations, with a very regular mesh in order to minimize its effect, the result is displayed in Figure 7. Of course, the results are not very good but the improvement between second and third order is tremendous, despite the crudeness of the mesh.

The scheme also works on nonlinear problems, for example $(f, g) = (u^2/2, u)$, where the initial condition is a cylinder. The results are displayed in Figure 8 for the mesh of 6. This result shows that one can handle nonlinear problems without major difficulty.

5. CONCLUSIONS

In this paper, we have sketched several strategies to construct very high-order schemes for scalar linear and nonlinear hyperbolic problems. Our preliminary results show that the method is promising, especially in terms of accuracy. We note that the stencil remains compact in space, contrary to ENO-like methods.

Many things remain to be done. We list a few. First, Equation (13) always leads to a nonlinear implicit equation. It is of fundamental importance to solve it well, otherwise accuracy is *not* guaranteed. It is important to develop efficient and reliable strategies for this problem. The solution of nonlinear hyperbolic systems must be investigated and those of parabolic problems like the Navier–Stokes equations. We are currently investigating these problems.

APPENDIX A: STABILITY ANALYSIS FOR RICCHIUTO'S N SCHEME

In this analysis, we assume a compactly supported solution. Starting from the N scheme (5), (7), we rewrite it as

$$|C_i|u_i^{n+1} + \sum_{j \neq i} c_{ij}(u_i^{n+1} - u_j^{n+1}) = |C_i|u_i^n$$

with $c_{ij} = \sum_{T \ni i} c_{ij}^T$ and $c_{ij}^T = \Delta t k_i^+ N k_j^-$. Here $|C_i| = \sum_{T \ni i} |T|/3$ is the area of the dual cell.

L^∞ stability: The scheme writes $Au^{n+1} = u^n$ with $a_{ii} = 1 + \sum_j c_{ij}/|C_i| > 0$, $a_{ij} = -c_{ij}/|C_i| < 0$ if $i \neq j$ so that A^{-1} is a matrix with positive entries. This guarantees the maximum principle.

Energy analysis: After multiplication by u_i^{n+1} and summation, we get

$$\mathcal{E}^{n+1} + \sum_i \sum_j c_{ij}(u_i^{n+1} - u_j^{n+1})u_i^{n+1} = \sum_i |C_i|u_i^n u_i^{n+1}$$

where $\mathcal{E}^{n+1} = \sum_i |C_i|(u_i^{n+1})^2$. Then we rearrange the second term, $\sum_i \sum_j c_{ij}(u_i^{n+1} - u_j^{n+1})u_i^{n+1} = \sum_T \sum_{i,j \in T} c_{ij}^T(u_i^{n+1} - u_j^{n+1})u_i^{n+1}$. The second summation $\sum_{i,j \in T} c_{ij}(u_i^{n+1} - u_j^{n+1})u_i^{n+1}$ can be rewritten as $\frac{1}{2} \sum_j k_j (u_j^{n+1})^2 + \frac{1}{2} \sum_{i,j \in T} c_{ij}^T (u_i^{n+1} - u_j^{n+1})^2$ because we have the relations $\sum_{j \neq i} (c_{ij}^T - c_{ji}^T) = k_i$. Coming back to the problem, we have

$$2\mathcal{E}^{n+1} + \sum_T \sum_j k_j^T (u_j^{n+1})^2 + \sum_{i,j} c_{ij}(u_i^{n+1} - u_j^{n+1})^2 = 2\sum_i |C_i|u_i^{n+1}u_i^n$$

Assuming now a *constant* velocity field, the second term vanishes and we get

$$\mathcal{E}^{n+1} \leq \sum_i |C_i|u_i^{n+1}u_i^n \leq 1/2(\mathcal{E}^{n+1} + \mathcal{E}^n)$$

so that $\mathcal{E}^{n+1} \leq \mathcal{E}^n$ unconditionally on Δt .

ACKNOWLEDGEMENTS

The research of N. Andrianov was supported by HYKE contract HPRN-CT-2002-00282.

REFERENCES

1. Deconinck H, Struijs R, Bourgeois G, Roe PL. Compact advection schemes on unstructured meshes. *Computational Fluid Dynamics VKI Lecture Series 1993–04*, 1993.
2. Abgrall R, Mezière M. Construction of second order accurate monotone and stable residual distribution schemes for unsteady flow problems. *Journal of Computational Physics* 2003; **188**(1):16–55.
3. Ricchiuto M, Abgrall R, Deconinck H. Construction of very high order residual distribution schemes for unsteady scalar advection: preliminary results. VKI Lecture Series 2003–05.
4. Abgrall R. Toward the ultimate conservative scheme: following the quest. *Journal of Computational Physics* 2001; **167**(2):277–315.
5. Abgrall R, Roe PL. Construction of very high order fluctuation scheme. *Journal of Scientific Computing* 2003; **19**(1–3):3–36.